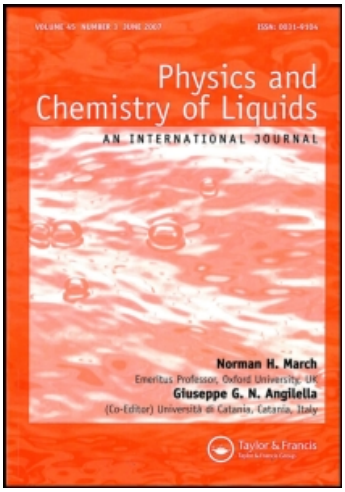

Physics and Chemistry of Liquids
Publication details, including instructions for authors and subscription information:
http://www.informaworld.com/smpp/title~content=t713646857

Physical Properties of Model Colloidal Liquids Using Brownian Dynamics Simulation

D. M. Heyes[a]; P. J. Mitchell[a]
[a] Department of Chemistry, University of Surrey, Guildford

To cite this Article Heyes, D. M. and Mitchell, P. J.(1995) 'Physical Properties of Model Colloidal Liquids Using Brownian Dynamics Simulation', Physics and Chemistry of Liquids, 30: 2, 113 — 134
To link to this Article: DOI: 10.1080/00319109508046430
URL: http://dx.doi.org/10.1080/00319109508046430

Phys. Chem. Liq., 1995, Vol. 30, pp. 113–134
Reprints available directly from the publisher
Photocopying permitted by license only

PHYSICAL PROPERTIES OF MODEL COLLOIDAL LIQUIDS USING BROWNIAN DYNAMICS SIMULATION

D. M. HEYES and P. J. MITCHELL

Department of Chemistry, University of Surrey, Guildford, GU2 5XH

(Received 16 February 1995)

Some aspects of the equilibrium and non-Newtonian behaviour of a free draining (Rouse level) Brownian Dynamics, BD, model colloidal liquids have been computed. Simulations have been carried out of spherical particles using the r^{-n} inverse power repulsive and hard-sphere interaction. The self-diffusion coefficients, linear dynamic viscosities, non-Newtonian viscosity behaviour and associated restructuring of the assembly have been computed.

Despite the very simple nature of the model, many of the computed properties follow closely the experimental data, giving at worst qualitative agreement. The model also obeys the Cox-Merz rule on rescaling either the frequency or shear rate.

Where the model does show significant differences from the experimental data, we can attribute this to the absence of many-body hydrodynamics in the model. For example, the long-time self-diffusion coefficient decreases with increasing volume fraction, but to a smaller extent than for the experimental systems. The magnitude of the viscosity and also the extent of liquid restructuring at high shear rates are other aspects of the model which probably suffer from the absence of many-body hydrodynamics.

KEY WORDS: Rheology, colloidal liquids, shear thinning, dynamic moduli.

1 INTRODUCTION

In a series of publications we have applied Brownian Dynamics computer simulation, BD, to investigate various aspects of the rheology, including the viscoelastic behaviour, of model colloidal liquids[1–10] using a free draining hydrodynamic model proposed by Ermak in 1975[11], which omits 'many-body hydrodynamics'. There are several alternative approaches currently being investigated by different groups to include these effects. Historically the first from Bossis and Brady[12], is an extension of Ermak and McCammon's diffusion tensor method[13], but extended to higher multipoles, including the so-called stresslet (the fluid stress integrated over the particle's surface) from which the shear stress in the sample can be formally defined (this is not developed in Ermak and McCammon's treatment). This approach treats the many-body hydrodynamics from the starting point of the 'far-field' Oseen tensor hydrodynamic solution for point particles, and then correcting for finite particle size. A number of other groups have proposed similar schemes, e.g., Ladd[14] and Cichocki *et al.*[15]. These methods are extremely time consuming to implement on a routine basis by virtue of matrix inversions required each step (an $O(N^3)$ operation), so only relatively small systems can be considered at present. In addition, for practical

reasons, only a finite number of the 'multipole' terms can be considered, and the expansion seriously breaks down when the particles approach closely (as they will in the course of their motion), so near-field squeeze film lubrication forces have to be 'added' into the model (these are based on an exact two-body solution of the fluid flow equations and can be incorporated on a pair-wise additive basis, to a good approximation, similar to the short-range colloid forces). An alternative, method for incorporating the far-field hydrodynamics has been proposed by Yuan and Ball[16] in which the 'creeping flow' fluid flow/pressure field equations for an incompressible fluid are solved numerically on an unconstrained ('Lagrangian') grid between the colloidal particles, subject to the boundary conditions being satisfied on the particle's surface. There are other approaches for treating the solvent, based on a lattice gas formalism, where the 'solvent particles' represent domains of solvent, either fixed on a grid ('on-lattice gas'[17]) or free to move continuously through space ('off-lattice gas'[18]). However, these lattice gas methods are radically different from the methods based around Ermak's algorithm, so we do not consider them further here.

Despite the obvious importance of including many-body hydrodynamics in the simulations, the Ermak BD technique reproduces many of the features of these real systems, such as hindered diffusion at high-volume fraction, non-Newtonian shear thinning in steady-state shear and strain amplitude shear 'softening' of the dynamic moduli in oscillatory shear. All of these effects take place at roughly the same values of strain rate and amplitude as with the experimental systems. Even, though there are no solvent-mediated many-body forces in the model, it works surprisingly well, indicating the importance of excluded volume effects in dense suspension rheology. Although the hydrodynamics-free (Ermak) Brownian dynamics, BD, algorithm will continue to have use as a convenient (analytically tractable) 'reference' model of a colloidal liquid, an increasing number of simulations will be carried out including some level of many-body hydrodynamics. Therefore, at this stage it is appropriate to take stock of the body of Ermak-based BD simulations and establish its strengths and weaknesses *vis à vis* the experimental systems. In this context, another test of the model, is in the relationship between the absolute value of the complex linear viscosity $|\eta^*(\omega)|$, (which can be obtained from the Fourier transform of the stress relaxation function in the linear response limit) and the shear-thinning viscosity $\eta(\dot{\gamma})$. Experimentally it has been found that these two functions are quite similar (especially for polymeric systems) and can be superimposed, which is called the Cox-Merz rule. Here we discuss the application of the simulation method to the Cox-Merz rule in some detail, as we have not considered it before. We compare the shear rate dependent viscosity obtained by finite shear rate simulations with the frequency dependent viscosity obtained from the time correlation functions (see below) to discover if the Cox-Merz rule applies to these model systems, and how the comparison varies with solids volume fraction.

The non-Newtonian (shear thinning) behaviour of colloidal liquids can be computed by applying a finite shear rate, $\dot{\gamma}$, to the model sample and then using the mechanical definition: $\eta = \langle\sigma\rangle/\dot{\gamma}$, where $\langle\sigma\rangle$ is the time-averaged shear stress. The problem with this technique is that at low shear rates the statistics deteoriate dramatically, so that it is difficult to extrapolate to zero shear rate to obtain an accurate value for the Newtonian viscosity. It is useful to be able to calculate the Newtonian

viscosity for a particular model system because it is central to any analytic interpretation of the non-Newtonian behaviour. In recent years we have made use of the Green-Kubo time correlation formula to calculate this viscosity in our Brownian Dynamics, BD, simulations. It has the advantage that it unambiguously produces the Newtonian viscosity, by being implicitly a linear response (and therefore infinitesimally small) shear rate method. In addition, if only the Newtonian viscosity is required, a single simulation is sufficient, whereas the non-equilibrium method, in which a finite shear rate is applied, requires at least several independent simulations at different shear rates to provide enough data points to extrapolate to zero shear rate (with the attendant problem of deciding on a suitable analytic form for extrapolation). In this respect, there are many similarities with the arguments made for equilibrium *vs.* non-equilibrium molecular dynamics in the 1980s[19].

An additional feature of this work is that we formally prove that the Green-Kubo time correlation function method can be applied to particles evolving using Brownian Dynamics equations of motion, although the derivation of this is implicit in some of the work of, e.g., Hess and Klein,[20]. We also investigate the effect of interaction potential and volume fraction on the short and long-time self-diffusion coefficients and compare with experiment.

2 GREEN-KUBO THEORY FOR COLLOIDS

Consider N colloidal particles and n solvent molecules ($n \gg N$). Under the assumption that the mass of the colloidal particle m far exceeds that of the solvent molecules and that the relaxation times of the solvent fluctuations are much shorter than those characterising the evolution of the structure of the macroparticle assembly, then the N–particle Fokker-Planck equation for the distribution function of the colloidal assembly, $f(\mathbf{\Gamma}, t)$ can be derived from the Liouville equation[21-23,42]

$$\frac{\partial f(\mathbf{\Gamma}, t)}{\partial t} = \hat{\Omega}(\mathbf{\Gamma}) f(\mathbf{\Gamma}, t) \tag{1}$$

where $\mathbf{\Gamma} = (\underline{p}_1 \ldots \underline{p}_N, \underline{r}_1 \ldots \underline{r}_N)$, are the momenta and positions of the colloidal particles. The operator, $\hat{\Omega}$ is given by,

$$\hat{\Omega}(\mathbf{\Gamma}) = -\sum_i^N \left(\frac{\underline{p}_i}{m} \frac{\partial}{\partial \underline{r}_i} + \underline{F}_i \frac{\partial}{\partial \underline{p}_i} \right) + \sum_i^N \frac{\partial}{\partial \underline{p}_i} \xi_{ij} \sum_{j=1}^N \left(\kappa_B T \frac{\partial}{\partial \underline{p}_j} + \frac{\underline{p}_j}{m} \right). \tag{2}$$

The Fokker-Planck operator, $\hat{\Omega}(\mathbf{\Gamma})$ involves the direct forces on the colloidal particles from the other colloidal particles, $\underline{F}_i$ and the second term in Eq. (2) is the solvent mediated interaction between the colloidal particles where ξ_{ij} is the friction tensor matrix. The frictional force on particle i from the velocities of all the other colloidal particles is given by.

$$\underline{F}_i^f = -\sum_{j=1}^N \xi_{ij} \frac{\underline{p}_j}{m} \tag{3}$$

The stationary solution of this is the canonical distribution function, $f_0(\mathbf{\Gamma}, t)$,[20]

$$f_0(\mathbf{\Gamma}, t) = \frac{1}{Z}\exp\left[-\beta\left(U(\mathbf{\Gamma}) + \sum_i \frac{p_i^2}{2m}\right)\right] \tag{4}$$

where U is the total interaction energy between the colloidal particles and the partition function Z normalises the distribution function so that the integral over all phase space is equal to unity. The time evolution of the phase space point is given by,

$$f(\mathbf{\Gamma}, t) = \exp(\hat{\Omega}(\mathbf{\Gamma}, t)) f(\mathbf{\Gamma}, 0). \tag{5}$$

where the Fokker-Planck operator. On the time-scale of the structural evolution of the colloidal particles the momenta of the colloidal particles can be projected out so that the $3N$-dimensional vector, $\underline{X} = (\underline{r}_1 \ldots \underline{r}_N)$ takes the place of $\mathbf{\Gamma}$, and the Fokker-Planck evolution operator is replaced by the Smoluchowski operator $\hat{\mathrm{D}}$,

$$\hat{D} = \sum_{i=1}^{N}\sum_{j=1}^{N} \frac{\partial}{\underline{r}_i} D_{ij}\left(\frac{\partial}{\partial \underline{r}_j} + \beta \frac{\partial U}{\partial \underline{r}_j}\right) \tag{6}$$

where $\beta = 1/\kappa_B T$ and D_{ij} is the mobility tensor. The distribution function $f(\mathbf{\Gamma}, t)$ is replaced by the N-particle configurational distribution function $P(\underline{X})$ with

$$P_0(\underline{X}) = \exp(-\beta U(\underline{X}))/Z(\beta) \tag{7}$$

Given any phase space variable, $A(\underline{X})$, we can write

$$A(t) = \int d\underline{X}\, A(\underline{X}) \exp(\hat{\mathbf{D}}t) P_0(\underline{X}), \tag{8}$$

If we apply an infinitesimal step in strain, $\gamma = \dot{\gamma}\delta(t - t_0)$ at $t = t_0$ then the difference in the value of the variable, $A(t)$, after the perturbation minus that in the absence of the perturbation, $A_0(t)$, is given by,

$$\delta A(t) = A(t) - A_0(t) = \int d\underline{X}\, A(\underline{X}) \exp(\hat{\mathbf{D}}_1 t) P_0(\underline{X}), \tag{9}$$

where the perturbation operator, $\hat{\mathbf{D}}_1 = \gamma\delta(t - t_0)\partial/\partial \underline{\underline{\epsilon}}$ and $\underline{\underline{\epsilon}}$ is the strain tensor. Adopting $A = \underline{\underline{\sigma}}$, the stress tensor, we have,

$$\delta \underline{\underline{\sigma}}(t) = \int d\underline{X}\underline{\sigma}(\underline{X})\, (\dot{\gamma}\delta(t - t_0)\, V\beta) \underline{\underline{\sigma}}\, P_0(\underline{X}), \tag{10}$$

where the $O(1)$ term disappears for the off-diagonal elements of $\underline{\underline{\sigma}}$ on the grounds of symmetry. Let us choose the element, σ_{xy},

$$\delta\sigma_{xy}(t) = \dot{\gamma}\delta(t - t_0)\, V\beta < \sigma_{xy}(t)\sigma_{xy}(0) >. \tag{11}$$

This is the linear stress relaxation function written as a time correlation function. The viscosity is given by the time integral of this function,

$$\eta = (\lim t \to \infty)\delta\sigma_{xy}(t)/\dot{\gamma} = V\beta \int_0^\infty dt' < \sigma_{xy}(t')\sigma_{xy}(0) >, \tag{12}$$

which is the Green-Kubo formula for the shear viscosity. Therefore, we have shown that, even though certain degrees of freedom have been projected out of the equations of motion, the Green-Kubo formulae can be used to determine the component of the transport coefficient associated with those degrees of freedom remaining in the equations of motion. We make use of the Green-Kubo formula for the shear viscosity in the next section.

3 SIMULATION DETAILS

The Ermak BD simulation method is used here to model near-hard sphere spherical colloidal particle liquids. We consider a cubic simulation cell containing particles interacting with an inverse power potential,

$$V(r) = \epsilon(\sigma/r)^n, \tag{13}$$

where σ is an effective particle diameter and r is the separation between the centres of the two model particles. We adopt the values, $\epsilon = \kappa_B T$ and n varying between 6 and 72, with most calculations using $n = 36$. The number of particles in the BD cells, N, was 256 for most of the simulations (although some were carried out using $N = 108$ and $N = 4000$), which has, from previous experience, been shown to give non-equilibrium behaviour of unassociating systems representative of the thermodynamic limit. The volume fraction used, $\phi = \pi\rho/6 = 0.3, 0.4, 0.45$ and 0.472, which is just below the maximum fluid density of a hard sphere fluid (0.494[25]). The computations were carried out using a neighbourhood table list to speed up the search for interacting particles. In the case of the $N = 4000$ simulations, link cells were used to construct the neighbourhood list.

The colloidal dynamics were modelled at a basic level using the Langevin equations, with an *assumed* extension to include interacting particles,[11], and the option of an applied shear flow (Non-equilibrium Brownian Dynamics),

$$\dot{\underline{r}}_i = \frac{\underline{p}_i}{m} + \underline{n}_x \dot{\gamma} r_{iy} \tag{14}$$

$$\dot{\underline{p}} = -\xi \underline{p} + \underline{R} + \underline{F}, \tag{15}$$

where $\underline{p}$ is the momentum of the Brownian particle, $\underline{R}$ is the Brownian force on the colloidal particle, which is represented by a normally distributed random number. $\underline{F}$ is the systematic or direct force between the colloidal particles (including any

external force). In the limit that the Browinian particle mass, M, is much larger than that of the solvent molecule, m, i.e., $M/m \gg 1$, the position update scheme proposed by Ermak in 1975 can be derived[6],

$$\underline{r}_i(t+h) = \underline{r}_i(t) + \frac{D_0}{k_B T}\,\underline{F}_i(t)h + \underline{\Delta r}_i(t,h) + \underline{n}_x \dot{\gamma} r_{iy} h \tag{16}$$

where $\Delta\underline{r}$ is the random displacement sampled from a gaussian distribution of zero mean and variance $<\Delta\underline{r}^2> = 6D_0h$, where $D_0 = k_BT/3\pi\sigma\eta_s = D_0/\xi$ is the self-diffusion coefficient for the colloidal particle at infinite dilution in a host solvent of viscosity η_s. As discussed in the introduction, the main limitation of this model is that it omits many-body hydrodynamics. The algorithm in Equation (16) is a modification of that proposed by Ermak[11], to include an imposed laminar shear flow with shear rate $\dot{\gamma}$ as a purely additive term.

A convenient characteristic time for structural evolution in the BD system in τ_r,

$$\tau_r = 3\pi\sigma\eta_s/4k_BT = a^2/D_0, \tag{17}$$

where $a = \sigma/2-$ is the radius of the particle. The random displacement in the x-direction is related to D_0, through

$$\langle \delta_x^2 \rangle = 2hD_0, \tag{18}$$

which was used to determine the magnitude of the time step, h. We first selected a desired root mean square displacement for each cartesian component, δ_m. This parameter is chosen to be small enough to prevent catastrophic overlap of particles and therefore unrealistically large interaction forces, and yet large enough so that a sufficient region of phase space can be explored in a reasonable simulation time to obtain good statistical averages. Equating $\langle \delta_x^2 \rangle$ (from (18)) to δ_m^2 yields a formula for h,

$$h = \delta_m^2/2D_0, \tag{19}$$

so that the time step is $\propto \delta_m^2$. We have found that a value of $\delta_x = 0.007 - 0.009\sigma$ was a convenient compromise value.

4 COMPUTED PROPERTIES

For the inverse power potentials considered here, all the equilibrium thermodynamic parameters and the linear moduli are proportional to the average interaction energy per particle, u, where

$$u = \frac{1}{2N}\sum_{i=1}^{N}\sum_{j\neq i}^{N}\langle V_{ij}(r_{ij})\rangle. \tag{20}$$

For example, the osmotic pressure is given by,

$$P = n\rho\langle u\rangle/3, \tag{21}$$

and the infinite frequency linear shear rigidity modulus, which is the storage modulus in the zero strain amplitude (γ_0) and infinite frequency limit, $G_\infty = G'$ ($\omega \to \infty$, $\gamma_0 \to 0$), is given by

$$G_\infty = (n^2 - 3n)\rho\langle u\rangle/15 \tag{22}$$

making use of the formula of Zwanzig and Mountain[27], omitting the kinetic term which is insignificant.

At finite concentration the diffusion process is slowed down by the interaction of the tagged particle with the other particles. The time-scale of velocity fluctuation of a single large mass, m, called the Brownian relaxation time is $\tau_B = m/\xi$. For times $t \gg \tau_B$ but $t \ll \tau_I$, the time it takes a particle to move a distance of order its diameter, the self-diffusion coefficient is D_S, the so-called short time self-diffusion coefficient. The hydrodynamic interactions occur on the time-scale as τ_B so these contribute to D_S. For $t \gg \tau_I$ a particle experiences a substantial change in the interaction force from the other particles and distorts the surrounding cage of colloidal particles as it moves through the liquid. This leads to a further decrease in the self-diffusion coefficient below that of D_S. The mean square-displacement of the particle in this time domain is termed the 'long-time' diffusion coefficient, D_L. The natural time scale for structural evolution of colloidal systems is a^2/D_0. The self-diffusion coefficients are computed from the mean square displacement, $W(t)$, which for a particular particle in the dispersion is,

$$W(t) = \frac{1}{6}\langle(\underline{r}(t) - \underline{r}(0))^2\rangle. \tag{23}$$

To improve statistical efficiency, the above formula is applied to each particle in the simulation in turn. The average $W(t)$ is obtained at the end of the simulation from the N individual $W(t)$s. The rate of change $W(t)$ gives the time dependent diffusion coefficient, $D(t)$,

$$D(t) = \frac{d\langle W(t)\rangle}{dt}, \tag{24}$$

which in the limit of $t \to \infty$ gives the so-called long-time self-diffusion coefficient. We find, as did Cichocki and Hinsen[15,29] that Eq. (24) converges more rapidly to the asymptotic limit than, $W(t)/t$, and therefore is a more reliable estimate of the long time self-diffusion coefficient as we are limited to a finite time duration for $W(t)$. We also have $D_0 = k_B T/\xi$, where $\xi = 3\pi\eta_s\sigma$ is the friction coefficient which provides a suitable quantity to normalise D_S and D_L.

The rheological behaviour of these systems is characterised in terms of the response of the stress tensor $\underline{\sigma}$, to shear straining. We have,

$$\underline{\sigma} = \frac{1}{v} \sum_{i=1}^{N-1} \sum_{j=i+1}^{N-1} \frac{\underline{r}_{ij}\underline{r}_{ij}}{r_{ij}} \frac{dV_{ij}}{r_{ij}}, \tag{25}$$

where v is the volume of the simulation cell. The Newtonian viscosity of a model MD computer liquid can be obtained using the Green-Kubo expression which includes a time-correlation function, $C_s(t)$, to be computed explicitly in the simulation and defined as

$$C_s(t) = \frac{v}{k_B T} \langle \sigma_{xy}(0)\sigma_{xy}(t) \rangle, \tag{26}$$

where $\langle \cdots \rangle$ indicates an average over time origins in equation (26). The Newtonian shear viscosity is given by,

$$\eta_0 = \int_0^{\infty} C_s(t)\, dt. \tag{27}$$

This method was first used by Levesque *et al.*[26] who applied it to Lennard-Jones liquids close to their triple point. The infinite frequency linear shear modulus is given by $G_\infty = C_s(0)$. The corresponding expression for the simple Langevin BD system is

$$\eta_0 - \eta_\infty = \int_0^{\infty} C_s(t)\, dt. \tag{28}$$

where η_∞ is the viscosity in the second Newtonian plateau. The present BD model only incorporates the thermodynamic interactions between the colloidal particles and ignores the many-body hydrodynamic solvent mediated forces. A measure of the contribution of many-body hydrodynamics to the total viscosity is given by the experimental value of the viscosity in the second Newtonian plateau, η_∞, which is entirely hydrodynamic in origin. The Equation (28) arises if we assume that the hydrodynamic contribution to the viscosity is equal to η_∞ at *all* shear rates, then the Green-Kubo formula in the present model gives the difference between the Newtonian viscosity η_0 (the zero-shear-rate limit) and η_∞. In the present context we do not have to know η_∞ as we are only interested in $(\eta_0 - \eta_\infty)$ which compares directly with the viscosity, η_0, that would otherwise be obtained doing the corresponding MD liquid simulation.

The Non-equilibrium Brownian Dynamics, NEMD, technique computes the viscosity at a finite shear rate, $\dot{\gamma}$, using Lees-Edwards sliding periodic boundary conditions,

$$\eta(\dot{\gamma}) - \eta_\infty = \langle \sigma_{xy}/\dot{\gamma} \rangle, \tag{29}$$

In the limit of $\dot{\gamma} \to 0$, the Green-Kubo and NEBD values for the viscosity should be the same. We quote the shear rate here in a dimensionless reduced form called the Peclet number, defined here to be, $Pe = \tau_r \dot{\gamma}$.

The linear dynamic moduli can be obtained by Fourier transformation of $C_s(t)$[35,37]. The storage modulus, G' and the loss modulus, G'' are given by,

$$G'(\omega) = \omega \int_0^\infty C_s(t) \sin(\omega t), \tag{30}$$

$$G''(\omega) = \omega \int_0^\infty C_s(t) \cos(\omega t), \tag{31}$$

The dynamics viscosity is, $\eta^*(\omega) = \eta'(\omega) - i\eta''(\omega)$ where $\eta'(\omega) = G''(\omega)/\omega$ and $\eta''(\omega) = G'(\omega)/\omega$. In the zero shear rate and zero frequency limit we have, $\eta'(\omega \to \infty) = \eta(\dot{\gamma} \to \infty) = 0$ in our model.

5 RESULTS AND DISCUSSION

A fundamental property of liquids is the self-diffusion coefficient of the component species. The short, D_S, and long-time, D_L, self-diffusion coefficients of the suspended particles in near-hard sphere colloidal liquids have been determined experimentally[32,33]. We computed both D_S and D_L for a range of colloid particle interactions, the numerical values of which are listed in Table 1. We have used an r^{-n} interaction as well as a hard-sphere interaction using an algorithm invented by Heyes and Melrose[30]. The Ermak BD model does show noticeable disagreement with experiment in the equilibrium short and long-time diffusion coefficients, as seen in

Table 1 Long-time self-diffusion coefficients D_L/D_0 as a function of volume fraction and n. *HS* stands for simulations using a hard-sphere Brownian Dynamics algorithms.

ϕ	$n=6$	12	18	36	72	*HS*
0.705	–	–	–	0.880	–	–
0.100	0.850	–	0.820	–	–	0.816
0.115	–	–	–	0.799	–	–
0.150	–	–	–	0.749	–	–
0.200	–	–	–	–	–	0.65
0.250	0.650	–	0.564	0.581	–	–
0.300	–	–	–	–	–	0.49
0.350	–	–	–	0.402	–	–
0.400	–	–	–	0.291	–	0.30
0.427	–	–	0.279	0.229	–	–
0.450	0.455	0.285	0.227	0.189	0.177	–
0.463	–	–	–	–	–	0.171
0.472	–	0.254	0.196	0.154	0.13	–
0.490	0.431	–	–	0.116	–	–
0.50	–	–	–	–	–	0.094

Figure 1(a). In the model we find, $D_S/D_0 = 1$, which is independent of ϕ, whereas the experimental evidence is for a steep decrease in this ratio with increasing volume fraction. The simulated D_L/D_0 does decrease with increasing ϕ, but the ratio is always above the experimental curve. Interestingly, it is statistically the same as the experimental D_S/D_0 over the entire volume fraction range. We note that, in Figure 1(a), the values of D for $n = 36$ and 72 are statistically indistinguishable from the hard-sphere data computed by Cichocki and Hinsen[15,29]. This suggests that the inverse power potential for $n > 36$ is a reasonable representation for the hard-sphere interaction in this context. As the interaction becomes softer then the value of D increases at fixed ϕ. It could be argued that the effective hard-sphere volume fraction of these different n fluids would not be equivalent to the value based on σ in the potential. To establish the influence of this, we have recomputed the volume fractions for each state point. An equivalent hard-sphere volume fraction was derived using the same value for the compressibility factor in the Carnahan-Starling equation of state[25] as that computed in the inverse power fluid simulation. In all cases the hard-sphere volume fraction was smaller than that based on the nominal σ in the potential. The differences are quite small for ϕ in excess of 0.4, but are significant for $\phi < 0.1$. The replotted D values are given in Figure 1(b), which reveals that even after this correction has been accounted for, the softer interactions **still** lead to higher diffusion coefficients, so this correction only has a minor effect.

In Figure 2, we show the normalised stress correlation functions, $C_s(t)$, for several $n = 36$ $N = 256$ states as a function of volume fraction, ϕ. These functions decay rapidly at short times, and then more slowly at longer times as volume fraction increases which reflects the slowing down of structural relaxation with increasing volume fraction. The *linear* G' and G'' for two of the volume fractions are presented in Figure 3(a) and Figure 3(b), respectively, for $\phi = 0.300$, 0.400 and 0.472. (The Fourier transforms were performed using Filon's method, which is necessary for $\omega a^2/D_0$ in excess of *ca.* 1000[31]). G' is the elastic component of the response and tends to G_∞ (given by Equation (22)) as $\omega a^2/D_0 \to \infty$. Using Equation (22) we have $G_\infty = 12.4, 33.1$ and 64.1 respectively. Figure 3 demostrates that these limits are reached in practice when $\omega a^2/D_0 \sim 2000$. The viscous component G'' reaches a maximum at $\omega a^2/D_0 \sim 800$ before declining with further increase in frequency (Figure 3(b)).

In Table 2 the computed shear viscosities are given as a function of shear rate and volume fraction. The Cox-Merz rule[34] is an empirical observation that the linear response $|\eta^*(\omega)|$ is the same as $\eta(\dot\gamma)$ and is found to work well for polymer solutions and melts. There is no theoretical justification for this 'rule' as the two processes of oscillation and shearing are quite different microscopically. The finite shear rate viscosity can be computed by BD on homogeneously shearing the contents of the cell of particles and also employing Lees-Edwards sliding image periodic boundary conditions. The $\eta^*(\omega)$ are computed numerically from the stress time correlation functions. Examples of $|\eta^*(\omega)|$ and $\eta^*(f\dot\gamma)$ are shown in Figure 4 for three volume fractions using an r^{-36} repulsive interaction. Although there is no strong evidence that real colloidal systems adhere to the Cox-Merz rule, these model systems do, in fact, show some degree of conformability in this respect if the dimensionless shear rate, $\dot\gamma a^2/D_0$, is scaled by a factor f. In this contest it is worth recalling that the BD

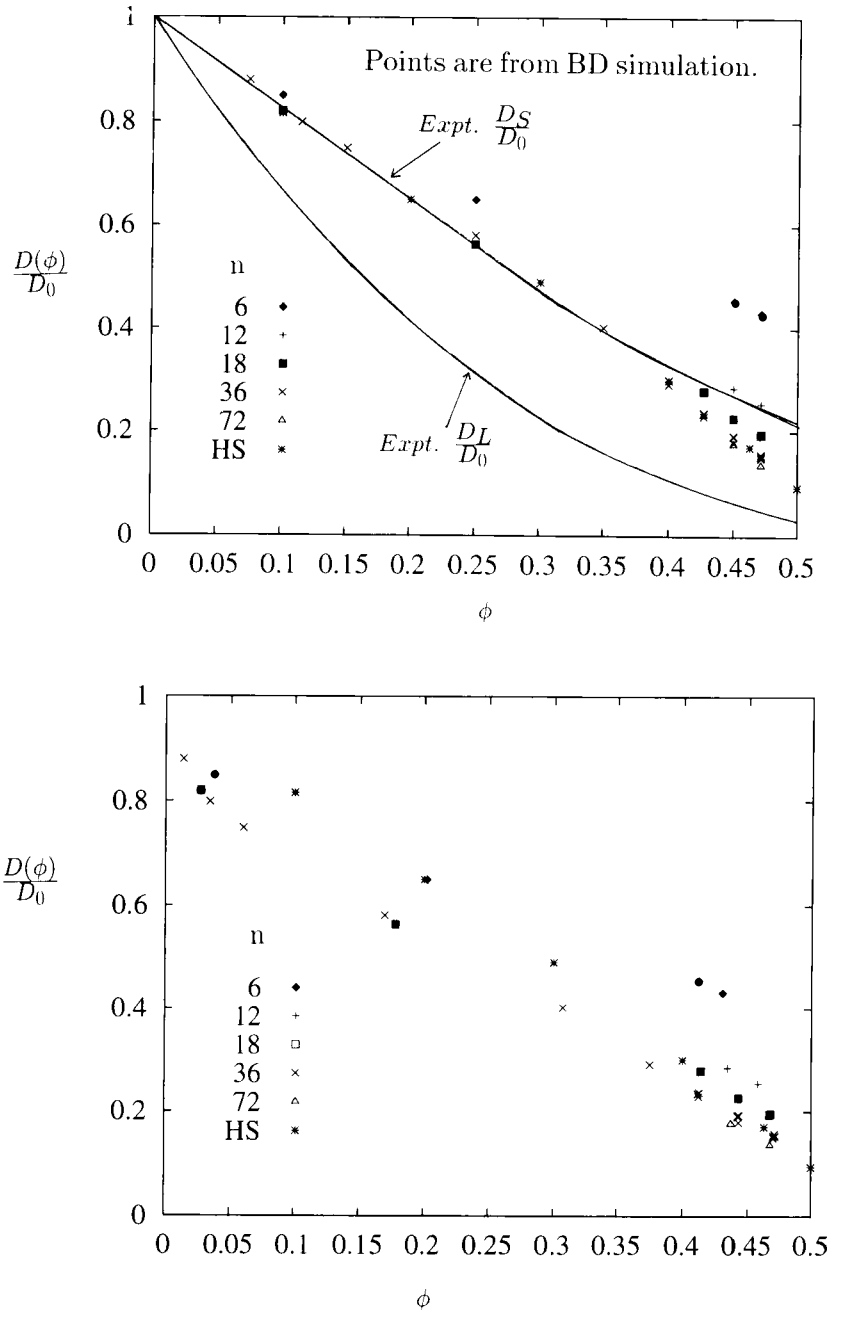

Figure 1 The diffusion coefficients for the BD model systems as a function of particle volume fraction using the inverse power potentials (r^{-n}) and *HS* (hard-sphere) interaction. The experimental data for D_S comes from [32] and D_L from [33]. Key: (a) we use the volume fractions based on σ from the potential, (i.e., $\phi = N\sigma^3/V$). and (b) we use a thermodynamic equivalent hard-sphere volume fraction.

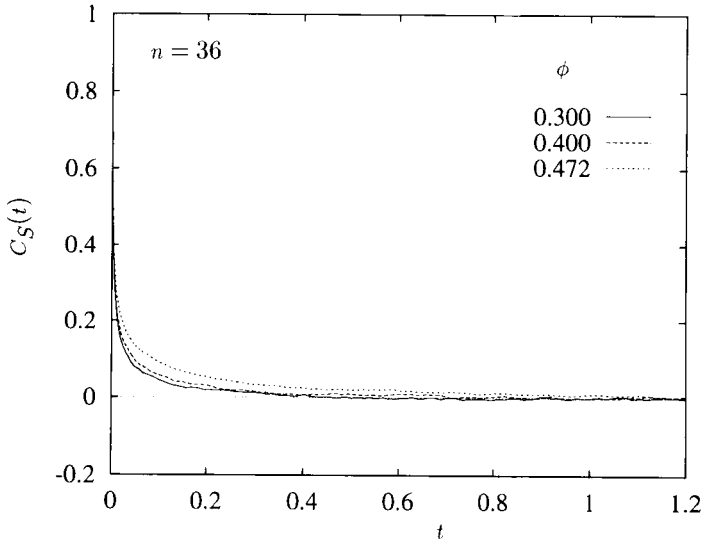

Figure 2 The shear stress time correlation functions for the equilibrium fluids using Equation (26) for the BD liquids.

model, however, predicts an infinite-frequency and infinite-shear rate viscosity which is zero, because both of these arise from fast solvent-mediated process between the colloidal particles, which are absent in the model.

The BD algorithm results in an ordering of the particles at high Peclet number ($Pe = \dot{\gamma}a^2/D_0$) into a semi-crystalline phase, called the 'string phase', first discovered

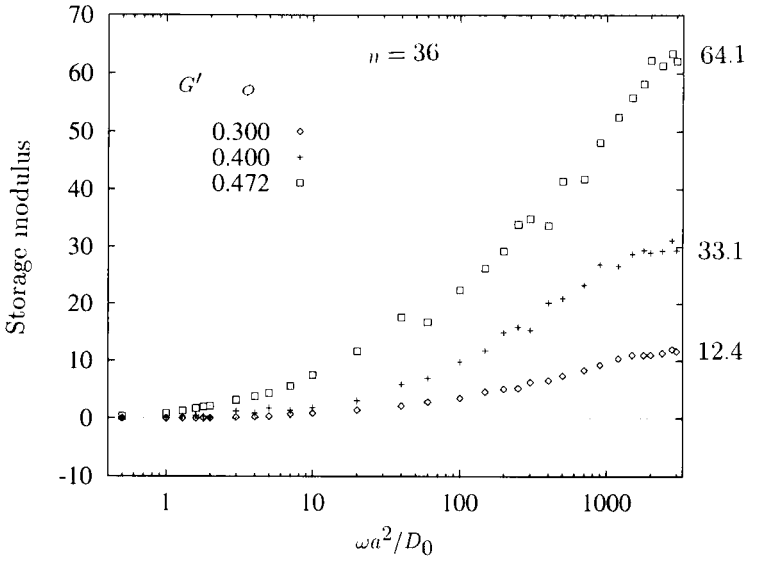

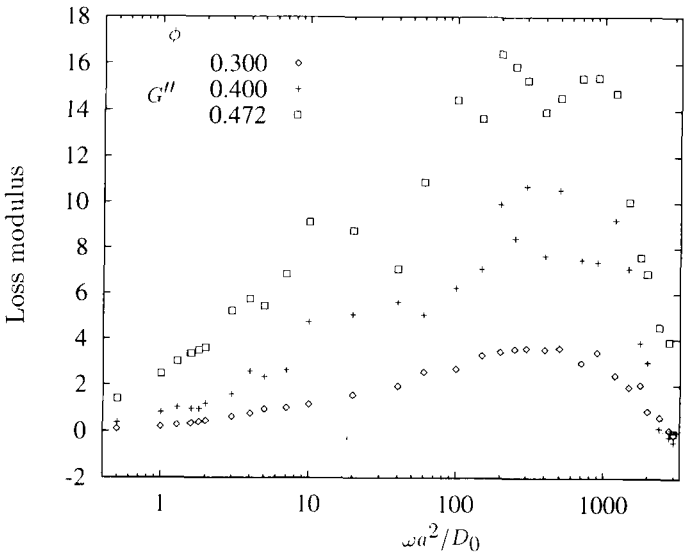

Figure 3 (a, b) The dynamic moduli for three volume fractions, $\phi = 0.300$, 0.400 and 0.472 using $N = 256$. (a) Storage Modulus G' and (b) Loss modulus G''. For (a) we also give, on the right of the figure, the value of G'_∞ using Equation (22).

by Erpenbeck in hard-sphere molecular dynamics simulations[43]. This is where the particles form into lines in the streaming (flow) direction. These lines or tubes of particles pack as a hexagonal close packed two dimensional lattice when viewed in cross-section. In order to minimise finite size effects, we have performed BD simulations on large systems of 4000 particles. Examples of these are given in Figures 5–7, showing particle assembly arrangements as shear rate is progressively increased. Figures 5(a)–(c) show particle projections on the three faces of the cell using a hard-sphere Brownian Dynamics[44] but otherwise conforming to the Ermak scheme. The gradient-vorticity yz plane shows the most structure. At $Pe = 20$ (Figure 5(a)) there is some evidence of a lamination of the particles into layers parallel to the flow-vorticity plane. At $Pe = 40$ (Figure 6(a)) the 'string' phase largely fills the simulation box, interestingly co-existing with a more amorphous region going through the middle of the box. This phenomenon has been observed in the past for equivalent Molecular Dynamics systems[38] and the 'nucleation' mechanism rationalised elsewhere[8]. As shear rate increases to $Pe = 200$ (Figure 7(a)) we see that most of this dislocation region has been annealed out. There have been a number of neutron[39-41] and light scattering studies of near-hard sphere colloidal liquids under shear in recent years, on both charge and sterically stabilised systems. Although, there is some evidence for shear-induced 'crystalline' ordering at high shear rate,[42], it would appear to be less pervasive and complete than that found by the shear-modified Ermak algorithm.

Table 2 Non-Newtonian viscosities obtained using Non-Equilibrium Brownian Dynamics. Key: Green-Kubo a) $N = 108$, and separate runs b) $N = 256$ and c) $N = 256$. The statistical certainty deteriorates dramatically as $Pe \to 0$, where $Pe = \dot{\gamma} a^2 / D_0$.

Pe / ϕ	$\eta(Pe) - \eta_\infty$ 0.300	$\eta(Pe) - \eta_\infty$ 0.400	$\eta(Pe) - \eta_\infty$ 0.450	$\eta(Pe) - \eta_\infty$ 0.472
0.0 a)	0.58	2.21	–	–
0.0 b)	0.57	2.05	–	6.64
0.0 c)	0.50	2.10	–	6.95
0.004	0.55663	–	–	–
0.005	–	–	6.5585	6.621
0.01	0.45183	1.9866	–	6.9425
0.02	–	–	4.1612	5.9197
0.04	0.48905	–	–	–
0.05	–	–	4.0199	5.9271
0.1	0.50009	1.7940	3.6520	5.5506
02	–	–	–	4.5427
0.3	–	–	3.0260	4.0176
0.5	–	–	–	3.3725
0.4	0.48365	–	–	–
0.7	–	1.1747	2.2934	–
1	0.40952	–	2.0675	2.4203
2.0	0.34673	–	–	1.8408
2.5	–	–	1.3574	–
3.0	–	–	–	1.5284
5	0.26797	0.64081	0.96624	–
10	0.2197	0.49595	0.66173	0.73512
15	0.19675	0.40871	0.43727	–
20	0.17518	0.34420	0.33114	0.35093
25	0.16136	0.28020	0.16909	–
30	0.15243	0.27173	0.13626	0.13188
35	0.13899	0.23448	0.10872	–
40	0.12667	0.13835	0.95433E-01	–
50	0.11146	–	–	–
60	0.91648E-01	–	–	–
70	0.78486E-01	–	–	–
80	0.65663E-01	–	–	–

6 CONCLUSIONS

In this work we have continued our Brownian Dynamics simulation studies of model colloidal liquids using the Ermak algorithm[11]. In particular, we have made a critical assessment of the model by making comparisons with experimental data on near-hard sphere colloidal liquids. We have found that the model does surprisingly well, bearing in mind its simplicity and indicating the importance of excluded volume effects. However, in certain properties there are significant discrepancies with experiment, which can be attributed directly to the omission of many body-hydrodynamics in the model.

Specifically, the first area of difference we would like to mention is in self-diffusion. The short-time self-diffusion coefficient in the model is, at *all* volume fractions, equal to the infinite dilution value of the experimental system. The corresponding experimental systems exhibit a dramatic decrease in the short-time self-diffusion

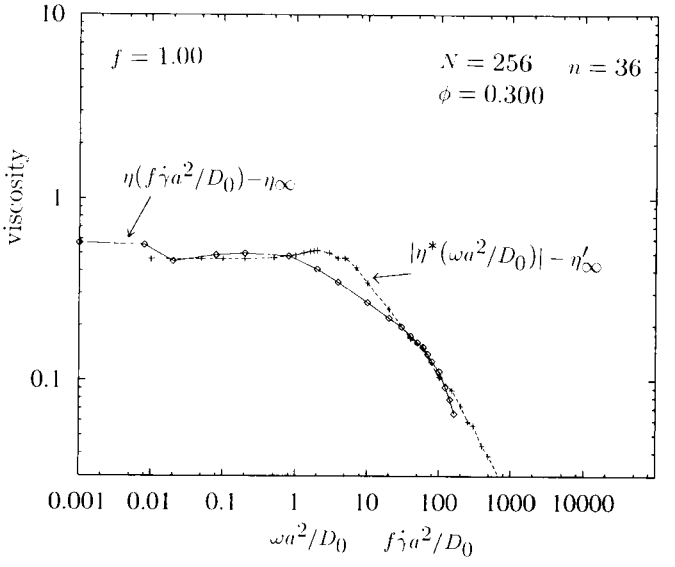

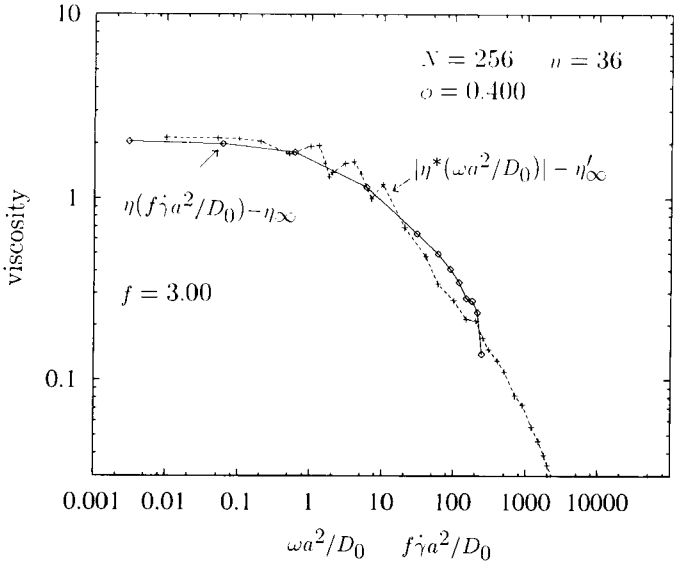

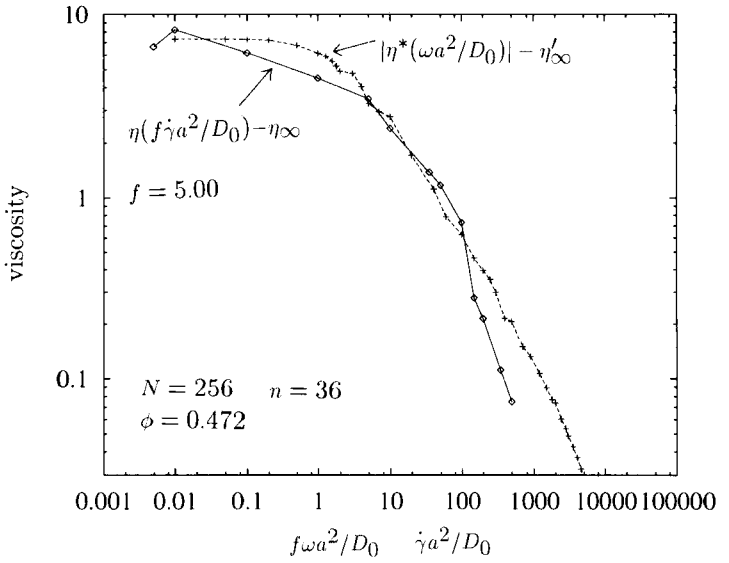

Figure 4 (a-c) A comparison between the absolute complex linear viscosity, $|\eta^*(\omega)a^2/D_0|$, obtained from the Fourier transformation of $C_S(t)$ and the shear rate dependent viscosity, $\eta(f\dot{\gamma}^2/D_0)$, where the non-dimensional shear rate has been scaled by the factor f. The simulations use the r^{-n} interaction with $n = 36$. Key: (a) $\phi = 0.300$, $N = 256$ and $f = 1.00$; (b) $\phi = 0.400$, $N = 256$ and $f = 3.00$; (c) $\phi = 0.472$, $N = 256$ and $f = 5.00$.

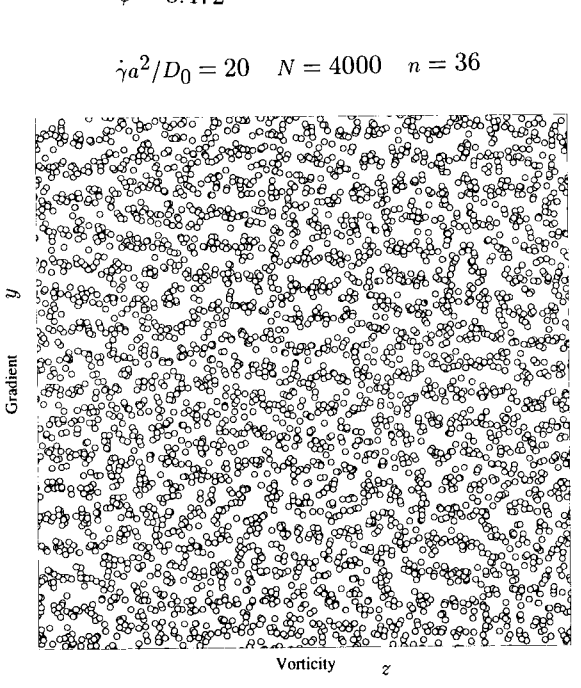

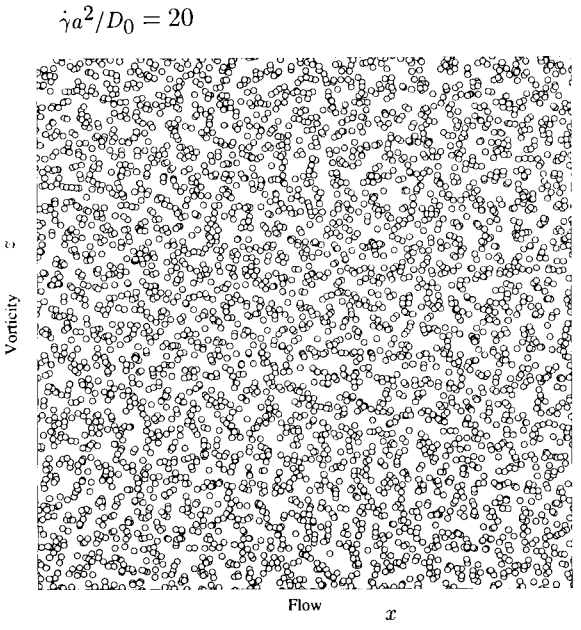

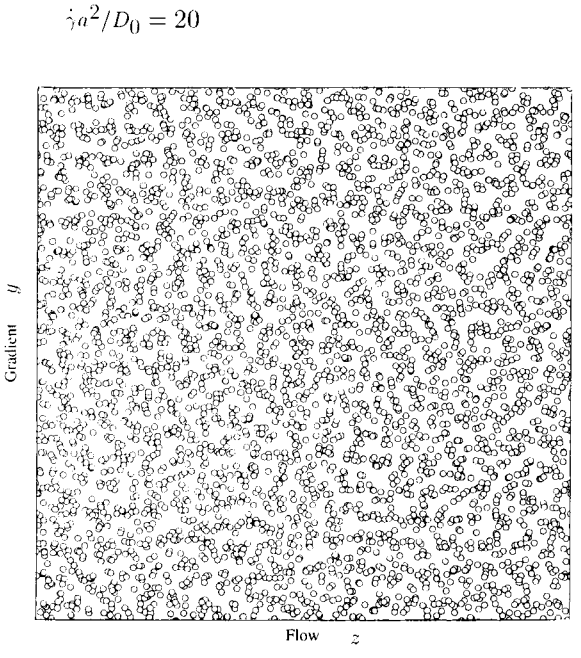

Figure 5 (a-c) A 'snapshot' structure of a state at a dimensionless shear rate of $\dot{\gamma}a^2/D_0 = 20$. The hard-sphere Brownian Dynamics algorith was used with $N = 4000$. The model coordinates are drawn at 10% of their true diameter to facilitate recognition of the structures formed. The particle coordinates are projected onto the following planes: (a) the gradient-vorticity (yz) plane, so that the viewing direction is along the shear flow (x) axis; (b) the xz plane and (c) the xy plane.

$\dot{\gamma}a^2/D_0 = 40$

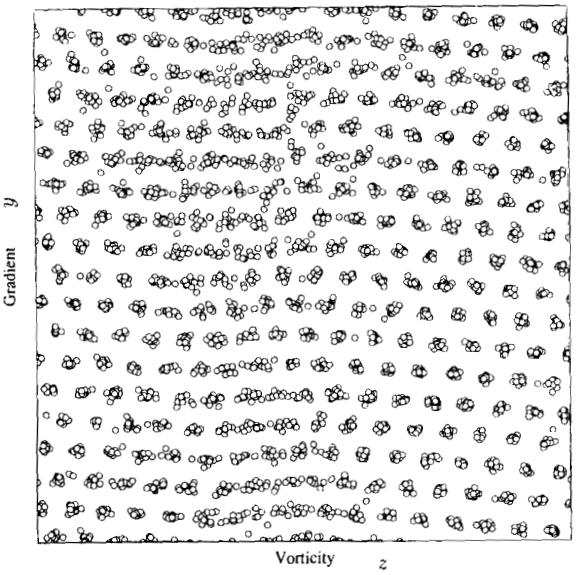

$\dot{\gamma}a^2/D_0 = 40$

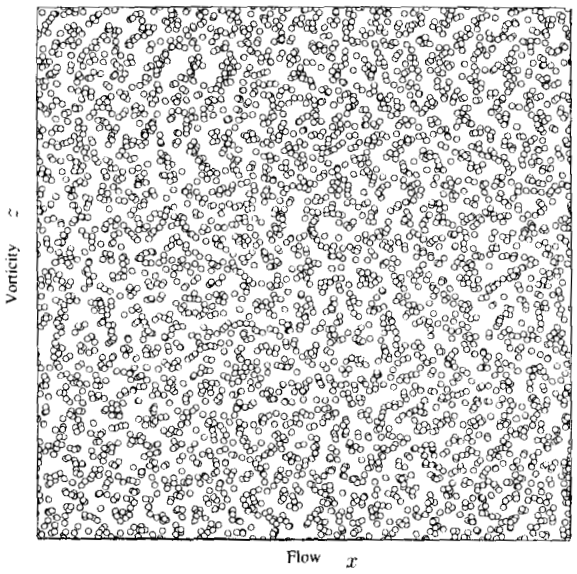

$\dot{\gamma}a^2/D_0 = 40$

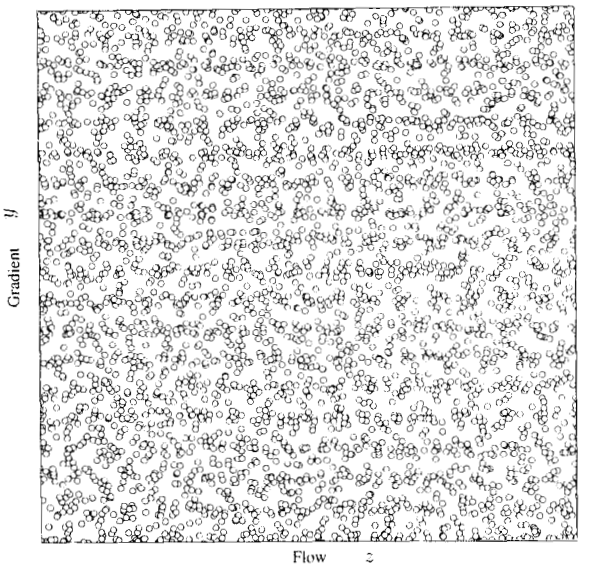

Figure 6 (a-c) As for Figure 5, except $\dot{\gamma}a^2/D_0 = 40$.

$\dot{\gamma}a^2/D_0 = 200$

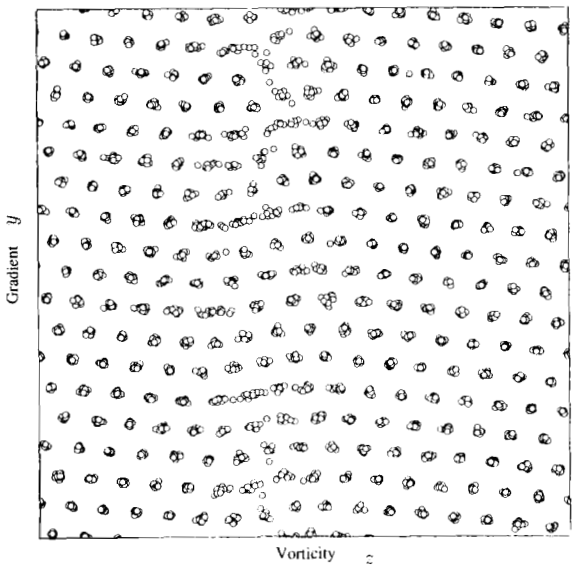

$\dot{\gamma}a^2/D_0 = 200$

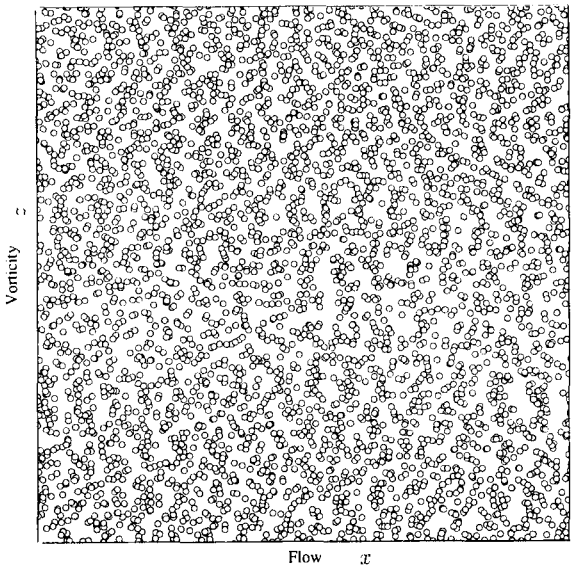

$\dot{\gamma}a^2/D_0 = 200$

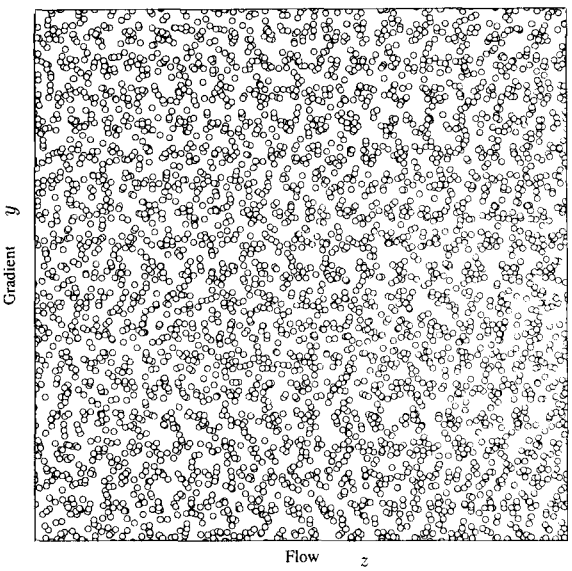

Figure 7 (a-c) As for Figure 6, except $\dot{\gamma}a^2/D_0 = 200$.

coefficient with increasing volume fraction. The long-time self-diffusion coefficient does decrease with increasing solids volume fraction, but to a less extent than in experimental systems. The solvent mediated many-body hydrodynamics in real systems slows down the rate of diffusion at very short times (compared with significant colloid particle displacement) because they act rapidly over a long-range ($\sim r^{-1}$ decay). Phenomena manifest on this timescale are beyond the scope of the present BD model. We suspect, that the long-time diffusion coefficient in our model is representing the **difference** between experimental long-time and short-time self-diffusion coefficients (*i.e.*, the resistance from the cage of colloidal particles on the mobility of a colloidal particle by virtue of the direct ('electrostatic') colloid-colloid interactions).

The second area where we note a difference between BD simulation and experiment is in the high shear rate viscosity and the high frequency linear response dynamic viscosity. The Ermak BD model cannot compute the absolute viscosity of the colloidal liquid at high frequency and/or high oscillation frequency. In the former case because the solvent-mediated many-body hydrodynamic forces dominate at high shear rates as the particles are forced together by the imposed flow field (the hydrodynamic forces go as $\sim (r-\sigma)^{-1}$ where σ is the hardsphere diameter). In the case of linear response oscillatory shear, the structure of the liquid is essentially that of the equilibrium liquid, so the colloidal molecules do not approach any closer on average. However, at high or 'infinite' frequency the timescales relevant to the suspension are those of the density fluctuations in the solvent and their interaction with the non-stationary framework of the colloidal particle assembly (just as for the short-time self-diffusion coefficient). Clearly, the simple BD model used here does not incorporate these effects, and consequently cannot obtain the 'infinite' limiting frequency dynamic rheology. Nevertheless, it has been found that both of these limiting cases can be corrected for, to a reasonable first approximation, by merely subtracting off the limiting values from the experimental data, suggesting that the hydrodynamic contributions are insensitive to frequency and shear rate.

The third area of possible discrepancy we have identified is in the semi-crystalline structures formed at high shear rate in the BD model, which persist indefinitely but for which there is no strong experimental evidence for.

Acknowledgement

P. J. M. thanks the Engineering and Physical Sciences Research Council of Great Britain and English China Clays (ECC) International Ltd for a research fellowship.

References

1. D. M. Heyes, P. J. Mitchell, P. B. Visscher and J. R. Melrose, *JCS Farad. Trans.*, **90**, 1133 (1994).
2. P. B. Visscher, P. J. Mitchell and D. M. Heyes, *J. Rheol.* **38**, 465 (1994).
3. D. M. Heyes and P. J. Mitchell, *JCS Farad. Trans.*, **90**, 1931 (1994).
4. S. M. Clarke, J. Melrose, A. R. Rennie, R. H. Ottewill, D. Heyes, P. J. Mitchell, H. J. M. Hanley and G. C. Straty, *J. Phys., Condens. Matter*, **6**, A333 (1994).
5. D. Heyes and P. J. Mitchell, *J. Phys.: Condens. Matter*, **6**, 6423 (1994).
6. D. M. Heyes and A. C. Brańka, *Phys. Chem. Liqu.*, **28**, 95 (1994).

7. D. M. Heyes, in 'Progress and Trends in Rheology', the proceedings of the 4th European Rheology Conference, Seville, Spain, September 4–9, 1994. ed. C. Gallegos, pp 657–659, (Darmstadt: Steinkopff, 1994, ISBN 3-7985-1005-9)
8. P. B. Visscher and D. M. Heyes, *J. Chem. Phys.*, **101**, 6096 (1994).
9. D. M. Heyes, *Adv. in Coll. & Interf. Sci.*, **51**, 247 (1994).
10. D. M. Heyes and A. C. Brańka, *Phys. Rev. E*, **50**, 2377 (1994).
11. D. L. Ermak, *J. Chem. Phys.*, **62**, 4189 (1975). *J. Chem. Phys.*, 4197.
12. L. Durlofsky, J. F. Brady and G. Bossis, *J. Fluid. Mech.*, **180**, 21 (1987).
13. D. L. Ermak and J. A. McCammon, *J. Chem. Phys.*, **69**, 1352 (1978).
14. A. J. C. Ladd, *J. Chem. Phys.*, **93**, 3484 (1990).
15. B. Cichocki, B. U. Felderhof, K. Hinsen, E. Wajnryb and J. Blawzdziewicz *J. Chem. Phys.*, **100**, 3780 (1994).
16. X. F. Yuan and R. C. Ball, *J. Chem. Phys.*, **101**, 9016 (1994).
17. A. J. C. Ladd, *Phys. Rev. Lett.*, **70**, 1339–1342 (1993).
18. P. J. Hoogerbrugge and J. M. V. A. Koelman, *Europhys. Lett.*, **19**, 155–160 (1992).
19. M. Ferrario, G. Ciccotti, B. L. Holian and J. P. Ryckaert, *Phys. Rev. E*, **44**, 6936 (1991).
20. W. Hess and R. Klein, *Physica A*, **105**, 552 (1981).
21. J. M. Deutch and I. M. Oppenheim, *J. Chem. Phys.*, **54**, 3547 (1971).
22. T. J. Murphy and J. L. Aguirre, *J. Chem. Phys.*, **57**, 2098 (1972).
23. B. J. Ackerson, *J. Chem. Phys.*, **64**, 242 (1976).
24. B. J. Ackerson, *J. Chem. Phys.*, **69**, 684 (1978).
25. L. V. Woodcock, *Ann. New York Acad. Sci.*, **271**, 274 (1981).
26. D. Levesque, L. Verlet and J. Kurkijarvi, 1973, *Phys. Rev. A*, **7**, 1690.
27. R. Zwanzig and R. W. Mountain, *J. Chem. Phys.*, **43**, 4464 (1965).
28. B. Cichocki and K. Hinsen, *Physica A* **166**, 473 (1990).
29. B. Cichocki and K. Hinsen, *Physica A* **187**, 133 (1992).
30. D. M. Heyes and J. R. Melrose, *J. Non-newt Fl. Mech.*, **46**, 1 (1993).
31. M. Abramowitz and I. A. Stegum, 'Handbook of Mathematical Functions', (Dover Pub., New York, 1970) p 890.
32. J.-F. Xue, E. Herbolzheimer, M. A. Rutgers, W. B. Russel and P. M. Chaikin, *Phys. Rev. Lett.*, **69**, 1715 (1992).
33. M. Medina-Noyola, *Phys. Rev. Lett.*, **60**, 2705 (1988).
34. D. Doraiswamy, A. N. Mujumbar, I. Tsao, A. M. Beris, S. C. Danforth and A. B. Metzner, *J. Rheol.*, **35**, 647 (1991).
35. B. Cichocki and B. U. Felderhof, *J. Chem. Phys.*, **101**, 7850 (1994).
36. T. S. Chow, *Phys. Rev. E.*, **50**, 1274 (1994).
37. N. J. Wagner, *Phys. Rev. E.*, **49**, 376 (1994).
38. D. M. Heyes, *J. Chem. Soc. Faraday Trans. II*, **82**, 1365 (1986).
39. P. Lindner, I. Marcović, R. C. Oberthür, R. H. Ottewill and A. R. Rennie, *Progr. in Coll. & Polym. Sci.*, **76**, 47 (1988).
40. C. G. de Kruif, J. C. van der Werff and S. J. Johnson, *Phys. Fluids A*, **2**, 1545 (1990).
41. J. C. van der Werff and C. G. de Kruif, *Progr. in Coll. & Polym. Sci.*, **81**, 113 (1990).
42. B. J. Ackerson and P. N. Pusey, *Phys. Rev. Lett.*, **61**, 1033 (1988).
43. J. J. Erpenbeck, *Phys. Rev. Lett.*, **52**, 1333 (1984).
44. D. M. Heyes and J. R. Melrose, 1993, *J. Non-newt Fl. Mech.*, **46**, 1 (1993).